

Transport Anisotropy of Ions in Sulfonated Polyimide Ionomer Membranes

Anne-Laure Rollet,* Olivier Diat,[†] and Gérard Gebel[†]

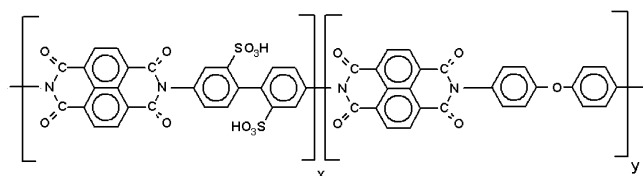
PCI/SI3M/DRFMC, CEA-Grenoble, 17 rue des Martyrs, 38054 Grenoble Cedex 9, France

Received: November 29, 2002; In Final Form: November 12, 2003

Transport processes of $\text{N}(\text{CH}_3)_4^+$ and Na^+ ions in sulfonated polyimide (sPI) ionomer membranes have been studied using three different techniques: pulsed field gradient NMR, a method using radiotracers, and conductivity. For $\text{N}(\text{CH}_3)_4^+$, the self-diffusion has been measured in the direction of membrane surface (parallel) and in the perpendicular direction (transverse), whereas for Na^+ only transverse self-diffusion has been measured. The effects of the equivalent weight and the length of the hydrophobic and hydrophilic sequence of the copolymer have been investigated. The length of hydrophilic sequence seems to have no influence on parallel diffusion and only a weak influence on transverse diffusion. The equivalent weight influences only transverse diffusion, albeit in a strong way. These effects are also observed in the conductivity experiments. The transport results testify to a multiscale foliated structure of the sulfonated polyimide ionomers.

1. Introduction

The emission of greenhouse gases, particularly those from automobile exhaust, are steadily increasing. The multiple consequences on health and nature prompt us to find a rapid solution to reduce or even eliminate the gas emissions. One way out is to turn toward fuel cells applications. However, some economic and technological barriers remain to be overcome before generalization of fuel cells on the world market. One of these barriers is the high cost of the Nafion ionomer membranes used nowadays. Numerous ionomer membranes have been developed as a substitute to Nafion, sulfonated poly(ether ether ketone),¹ sulfonated polysulfone,² and others, but their life span and stability in fuel cells are often insufficient. More recently,^{3,4} a new kind of ionomer has been proposed, the sulfonated polyimide (sPI), which is a kind of sequenced block copolymer. Its advantages are the following: high ionic selectivity, high conductivity,⁵ interesting gas permeation properties,⁶ and weak geometrical variation during swelling–deswelling cycles because of a high vitreous transition temperature (T_g about 270 °C). Moreover, it is possible to vary the length of the hydrophilic and of the hydrophobic sequences in the polymer chains and also to vary the ionic charge capacity. This is of great interest in the fundamental studies on the relation between the polymer chain primary structure and the structural and dynamic properties of the membrane. The first sPI that had been proposed was of phthalic kind but its life span in fuel cells (at 80 °C) was less than 10 min. More recently,^{3,4,7,8} the synthesis of naphthalenic sPI has permitted achievement of life span exceeding 3000 hours at room temperature. In this paper, we are interested in the latter system with the following chemical formula:



* To whom correspondence should be addressed. Current address: CRMHT-CNRS, 1D avenue de la Recherche Scientifique, 45071 Orléans cedex, France. Fax: 33 2 38 63 81 03. Tel: 33 2 38 25 76 82. E-mail: rollet@cnrs-orleans.fr.

[†] E-mail addresses: odia@cea.fr; ggebel@cea.fr.

In this paper, we have studied the ionic self-diffusion and the conductivity in naphthalenic sPI ionomer membranes neutralized by $\text{N}(\text{CH}_3)_4^+$ and Na^+ .

2. Experimental Section

2.1. Membrane Preparation. The polymers were synthesized at the LMOPS (CNRS, Vernaion, France) using a two-step method, which has been described in detail in previous publications.^{3,4} The average number of sulfonated monomers per ionic sequence is noted by X . The ion content in the polymer chains is defined through the equivalent weight, noted EW throughout the paper and defined as the mass of polymer per mole of SO_3^- charges. Several block sizes ($X = 3, 5, 7$, and 9) and two equivalent weights ($\text{EW} = 792$ and 504 g/equiv) have been used to study their influences on the transport properties of sPI membranes.

The polymer membranes have been prepared by spreading a solution of sPI in metacresol over a hot plate. When dried, the membranes were released by immersion in water. Then, they were placed in reflux in boiling methanol to remove the leftover metacresol. Finally, they were acidified using a 0.1 M HCl solution and carefully rinsed.

Then, the membranes were neutralized by Na^+ or $\text{N}(\text{CH}_3)_4^+$ ions: the membranes were immersed in highly concentrated solutions of NaCl or $\text{N}(\text{CH}_3)_4\text{Cl}$, and after a sufficient time they were rinsed several times with pure water.

The water content of sPI membranes has been measured by weighing.

2.2. NMR. The self-diffusion coefficients of $\text{N}(\text{CH}_3)_4^+$ ions have been measured by pulsed field gradient spin–echo (PFGSE) NMR.⁹ The principle can be briefly recalled: at time $t = 0$, the spins are labeled with respect to their position (in the collinear direction of the magnetic field \mathbf{B}_0 in our case) by applying a pulse of magnetic field gradient; after an evolution time Δ , a second pulse of magnetic field gradient opposite to the first one is applied. The second pulse cancels the effect of the first one, unless the spins have moved during the time Δ ; in that case, the second gradient pulse does not refocus all of the spins, and the echo signal is less intense. This decrease is a function of the self-diffusion coefficient D . In this study, we have used a BPP LED PFG sequence (bipolar pulse pairs longitudinal eddy current delay pulsed field gradient) that has

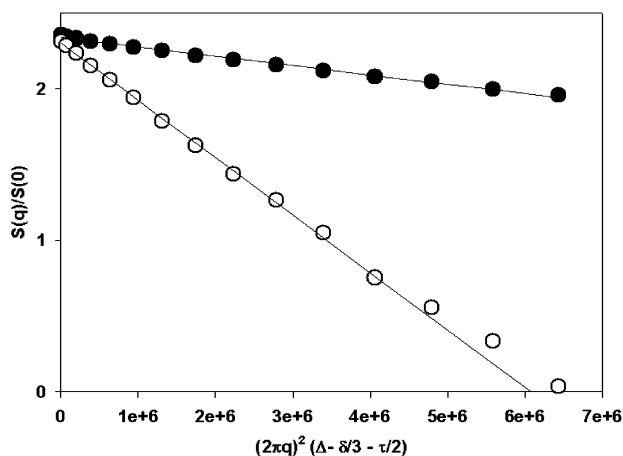
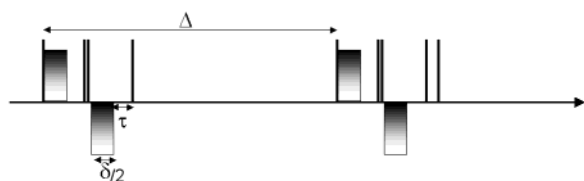


Figure 1. Decrease of NMR signal versus the gradient strength in the parallel direction (○) and in the transverse direction (●). The lines are the linear regression results.

been developed by Wu et al.¹⁰ from the sequence of Cotts et al.¹¹ There are some difficulties in measuring the self-diffusion coefficient of big molecules and of species confined in porous media such as ionomer membranes. First of all, the D values are more than 1 order of magnitude smaller than those in nonconfined solutions, and the use of a high gradient is therefore required to achieve a sufficient decrease of the echo, $S(q)$, compared with $S(0)$. The high gradient may lead to eddy currents. Second, the relaxation times in porous media are often very short, with $T_1 \gg T_2$, which can make it impossible to measure transport coefficients, as no signal can be measured. The advantages of the sequence used here are less intense eddy currents and the echo being stored longitudinally during Δ (according to T_1). This NMR sequence is represented as follows:



In this diagram, a single line represents a 90° pulse and a double line a 180° pulse. The gradient pulses are represented by the rectangle in gray shading.

The signal measured using this sequence is

$$S(q) = S(0) \exp[-4\pi^2 D q^2 (\Delta - \delta/3 - \tau/2)] \quad (1)$$

with $q^2 = (\gamma^2 g^2 \delta^2)/(4\pi^2)$ where g is the gradient strength and γ the gyromagnetic ratio of the proton.

This sequence is repeated with 15 gradients of increasing strength, and D is obtained by a fit of $\ln[S(q)/S(0)]$ versus q^2 (see Figure 1).

The gradient strength g ranged from 0 to 30 G/cm with an application time δ of 4.5 ms. The measurements have been performed using a VARIAN unity+ 500 MHz spectrometer. A 4×4 cm² piece of membrane was rolled and put in a NMR tube of 4 mm in diameter; the self-diffusion coefficient was then measured in the direction parallel to the membrane surface (D_{Pr}). For the membrane $X = 9$ and $EW = 792$ g/equiv, the transverse self-diffusion coefficient (D_{Tr}) has been also determined; in this case, disks of membrane have been stacked in the NMR tube. In all of the experiments, the temperature was set at 298 K by a flow of gas. For NMR experiments, the ionomer membranes have been rinsed several times in D₂O.

These NMR measurements have thus been performed for ionomer without added salt.

2.3. Radiotracers. The radiotracer method used in the present work to determine the $N(\text{CH}_3)_4^+$ and Na^+ self-diffusion coefficients in sPI membranes is based on the rotating electrode principle. A detailed description of this method has been given in a previous publication.¹² However, the principle can be briefly described: a circular piece of membrane was glued on a Plexiglas cylinder with a mastic. The cell was first immersed into an electrolyte solution of a given molality, m . After a sufficient time, it was introduced into a radiolabeled electrolyte solution of the same composition. When equilibrium was reached, the cell was mounted on a rotating electrode spindle and immersed into a nonradioactive solution of molality m . Then successive aliquots of this solution were taken as a function of time, and corresponding radioactivity is measured. The transverse self-diffusion coefficient, D_{Tr} , is determined by fitting the ratio of inner to outer radioactivity as a function of time using the following expression.

$$P(t') = (4t'/\pi)^{1/2} - [1 - Y(\lambda t'^{1/2})]/\lambda \quad (2)$$

where

$$t' = t(D_{Tr}/e^2)$$

$$Y(x) = \exp(x^2) \operatorname{erfc}(x)$$

$$\lambda = K^{-1}(eD_0/(p\delta D_{Tr}))$$

$$\delta = 1.612(\nu/\omega)^{1/2}/(\nu/D_0)^{1/3}$$

e being the membrane thickness, D_0 the self-diffusion coefficient of ions in the external solution, and p the porosity of the membrane.

Contrary to the case for NMR and conductivity experiments, the radiotracer experimental setup does not allow us to study the system in the absence of salt. In that case, one follows the exchange of radiolabeled species contained in the membrane with nonradiolabeled species contained in the external solution; in this study, the external solution concentration was thus 10^{-1} mol/L. For another, the experimental setting allows one to measure the transverse self-diffusion coefficient.

The whole system was thermostated at 298 K during the experiment. The experiments have been done several times (more than three times), and the values reported in Table 1 are the average. The standard deviation is about 20% for $N(\text{CH}_3)_4^+$ ions and 10% for Na^+ ions. The radiolabeled $^{14}\text{CH}_3\text{N}(\text{CH}_3)_3^+$ species are β emitters; the aliquots (50 μL) were then mixed with 5 mL of Aqualyte JT Baker scintiller liquid. The radioactivity was counted by Packard Tri-Carb 2100CR. For $^{22}\text{Na}^+$ (γ emitters), the aliquots (200 μL) were directly counted with Packard Cobra II.

2.4. Conductivity. The conductivity experiments have been carried out with a mercury cell,¹³ as previously described.¹⁴ A piece of swollen membrane separates two compartments filled with Hg; the surface in contact with these electrodes is 0.383 cm². The conductivity is thus measured in the transverse direction. A Paar 273 potentiostat and a Solartron SI1255 frequency analyzer were used for impedance measurements. The spectra were recorded over a frequency ranging from a few hertz to several hundred of kilohertz. The value of the membrane resistance was determined when the imaginary part of the impedance is equal to zero (frequency about 50 000 Hz).

TABLE 1: Values of the Transport Coefficient (the Subscript Refers to the Direction; Tr = transverse, Pr = Parallel), the Conductivity χ_{Tr} , the Diffusion Coefficient as Deduced from the Conductivity, and the Nernst–Einstein Equation, $D\chi_{\text{Tr}}$, the Parallel Self-Diffusion Coefficient Measured by the PFGSE NMR Technique, D_{Pr} , and the Self-Diffusion Coefficient Measured by the Radiotracer Technique, D_{Tr}

EW	X	χ_{Tr} $\times 10^3 \text{ S/cm}$ Na^+	χ_{Tr} $\times 10^3 \text{ S/cm}$ $\text{N}(\text{CH}_3)_4^+$	$D\chi_{\text{Tr}}$ $\times 10^{11} \text{ m}^2/\text{s}$ Na^+	$D\chi_{\text{Tr}}$ $\times 10^{11} \text{ m}^2/\text{s}$ $\text{N}(\text{CH}_3)_4^+$	D_{Tr} $\times 10^{11} \text{ m}^2/\text{s}$ Na^+	D_{Tr} $\times 10^{11} \text{ m}^2/\text{s}$ $\text{N}(\text{CH}_3)_4^+$	D_{Pr} $\times 10^{11} \text{ m}^2/\text{s}$ $\text{N}(\text{CH}_3)_4^+$
504	5	3.7	1.3	3.3	1.3	3.4	0.91	2.5
504	9	4.5	1.6	4.1	1.5	3.9	1.0	3.2
792	3	1.4	0.18	2.1	0.27	0.82	0.16	
792	5	1.1	0.22	1.6	0.26	0.93	0.15	
792	7	0.93	0.23	1.4	0.36	0.63	0.16	2.9
792	9	0.67	0.17	1.0	0.27	0.58	0.17	2.3

The conductivity measurements have been performed for ionomer neutralized by Na^+ or $\text{N}(\text{CH}_3)_4^+$ ions and without added salt. As for radiotracer experiments, the experiments have been performed several times, and the values reported in Table 1 are the average over at least four measures. The standard deviation σ is about 10% for $\text{N}(\text{CH}_3)_4^+$ ions and 20% for Na^+ ions.

3. Results and Discussion

3.1. NMR. Figure 2 illustrates the variation of the $\text{N}(\text{CH}_3)_4^+$ self-diffusion coefficient in sPI ionomer membranes as function of Δ ; D decreases with Δ until 1 s and then remains constant. For each membrane, that is, $X = 5$ and 9 for EW = 792 g/equiv and $X = 7$ and 9 for EW = 504 g/equiv, the same kind of dependence of D versus Δ has been observed. This behavior is characteristic of restricted diffusion.^{15–17} In porous media, the self-diffusion coefficient D depends on the window time (noted here as Δ) during which the measurements are performed. Therefore, the values are apparent self-diffusion coefficients. At very short time intervals, the molecules do not have enough time to explore the structure and encounter the walls of the pores. D is then equal to D_0 , the self-diffusion coefficient for unconfined solution. For longer intervals, the molecules encounter the walls, and as their path is restricted, D is smaller than D_0 . The bigger Δ is, the smaller D becomes, until Δ gets sufficiently large for the molecules to explore the whole representative volume of sample; the effect of the structure on the diffusion is averaged, and D no longer depends on Δ . Between these two limits, several features can be observed depending on the complexity of the system and its different levels organization. In this paper, we will focus on the study of this plateau value of the self-diffusion coefficient based on the membrane's orientation and structure. The complete analysis of the dependence of D_{Pr} on Δ will be detailed in a future

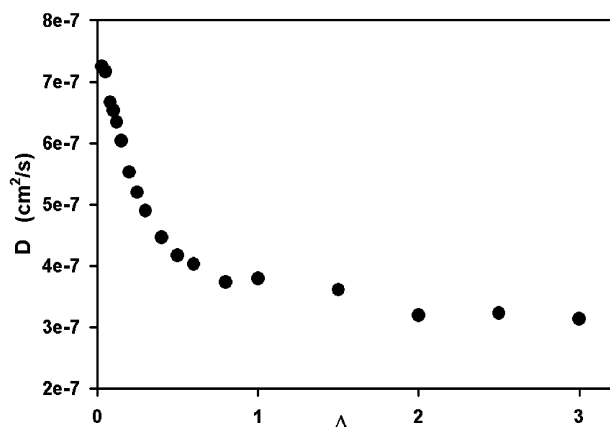


Figure 2. Typical variation of the self-diffusion coefficient of $\text{N}(\text{CH}_3)_4^+$ ions in sPI membrane versus the observation time Δ as measured by PFGSE NMR.

publication, numerical simulations being required. Using the plateau values, we can calculate a characteristic length of the representative volume of the structure: for $\Delta = 1 \text{ s}$ and $D_{\text{Pr}} = 10^{-11} \text{ m}^2/\text{s}$, $L = (2D\Delta)^{1/2} = 4 \mu\text{m}$. It appears then that there is no structure of characteristic length larger than $4 \mu\text{m}$ that disturbs the ion transport in sPI membranes.

In Figure 3, the parallel self-diffusion coefficients D_{Pr} of $\text{N}(\text{CH}_3)_4^+$ (plateau values) are plotted as a function of the block size X for sPI membranes of EW = 792 and 504 g/equiv. The number of data points available is small compared with those obtained with the radiotracer technique and conductivity, because the relaxation times (T_1 and T_2) of the ^1H of $\text{N}(\text{CH}_3)_4^+$ in sPI membranes were short (T_1 ranged from 2 s to 200 ms and T_2 ranged from 20 to 5 ms) and in some instances so short that the measurement of D by the PFGSE NMR technique was impossible. No relevant variation is observed in Figure 3; it seems that D_{Pr} of $\text{N}(\text{CH}_3)_4^+$ is influenced neither by X nor by EW. As far as EW is concerned, this is a rather surprising result because EW is expected to act upon the porosity of the membrane and as a consequence upon its tortuosity. For perfluorosulfonated ionomer membranes, an influence of EW has been observed on the transverse conductivity¹⁸ and self-diffusion coefficient of counterions.^{19,20}

The self-diffusion coefficient of $\text{N}(\text{CH}_3)_4^+$ ions has been also measured by PFGSE NMR in the transverse direction for one sPI membrane (with EW = 792 g/equiv and $X = 9$); D_{Tr} is about 4 times smaller than D_{Pr} (see Figure 3 and Table 1). The NMR measurements reveal a strong anisotropy of the transport properties of sPI membranes. This anisotropy was expected because (1) small angle scattering (X-ray and neutrons) experiments had revealed a strong anisotropy of the structure²¹ in the

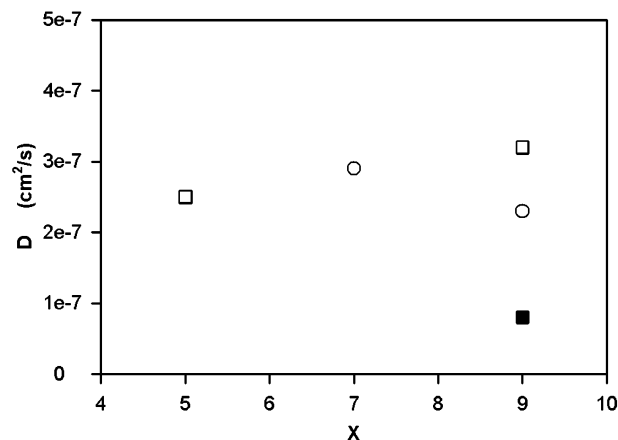


Figure 3. Parallel self-diffusion coefficient of $\text{N}(\text{CH}_3)_4^+$ ions in sPI membrane measured by PFGSE NMR versus the block size X for membrane with EW = 792 g/equiv (\circ) and membrane with EW = 504 g/equiv (\square). The transverse self-diffusion coefficient of the membrane with EW = 504 g/equiv and $X = 9$ is also reported (\blacksquare).

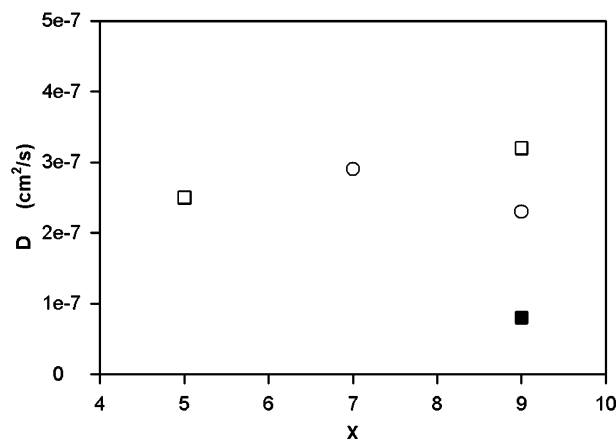


Figure 4. Transverse self-diffusion coefficient of $\text{N}(\text{CH}_3)_4^+$ ions in sPI membrane measured by the radiotracer method versus the block size X for membrane with $\text{EW} = 792$ g/equiv (○) and membrane with $\text{EW} = 504$ g/equiv (□).

space scale of 1–100 nm and (2) the microscopy studies show anisotropic structure at the micrometer scale.²²

To get information on the packing in sPI membranes, these NMR results can also be compared with those obtained with a well-defined confined medium. The ratio of the plateau value of the self-diffusion coefficient over the extrapolated value at $\Delta = 0$ can be compared to those obtained in simpler systems, such as a packed glass balls. For packing of different polystyrene and glass spheres ranging from 30 to 200 μm in diameter,^{23,24} this ratio is about 0.7. For a gel²⁵ of Laponite (discoid synthetic clay of 300 Å in diameter and 10 Å in thickness) with a volume fraction equal to 0.05, the suspension is isotropic and the ratio is also about 0.7, but for a more concentrated gel with volume fraction equal to 0.15, a nematic organization occurs and the ratio is 0.3 in the transverse direction and 0.6 in the parallel direction. In the case of a sPI membrane, it is about 0.4. This comparison seems to indicate that the concentration of objects of micrometer size in the sPI membrane is around 0.15 in volume fraction.

3.2. Radiotracers. The transverse self-diffusion coefficients D_{Tr} of $\text{N}(\text{CH}_3)_4^+$ determined from radiotracers measurements are plotted versus X in Figure 4, and the corresponding values are reported in Table 1. The striking feature is the strong difference between the values of D_{Tr} obtained for membranes with $\text{EW} = 792$ g/equiv and those obtained for membranes with $\text{EW} = 504$ g/equiv: they are separated by a factor 5. This is contrary to D_{Pr} results (NMR) since no significant difference was revealed. The influence of X on D_{Tr} is very weak: no variation of D_{Tr} versus X for $\text{EW} = 792$ g/equiv membrane and a very small increase for $\text{EW} = 504$ g/equiv.

The transverse self-diffusion coefficients of Na^+ ions have been also measured using this technique. In the case of Nafion membrane, it has been shown that Na^+ ions and $\text{N}(\text{CH}_3)_4^+$ ions exhibited different transport properties;^{12,26,27} therefore, it would be interesting to know whether such a difference occurs also in sPI membranes as their structural and swelling properties are very different from those of perfluorosulfonated ionomer membranes. The D_{Tr} values of Na^+ ions are plotted in Figure 5 versus the block size X . The same feature as for $\text{N}(\text{CH}_3)_4^+$ occurs here: a strong influence of EW and a very weak one of X . The effects of EW and X are the same with Na^+ and with $\text{N}(\text{CH}_3)_4^+$ ions.

A comparison of the self-diffusion coefficients in sPI membranes with those in nonconfined solution may give valuable information on the polymer structure. The ratios

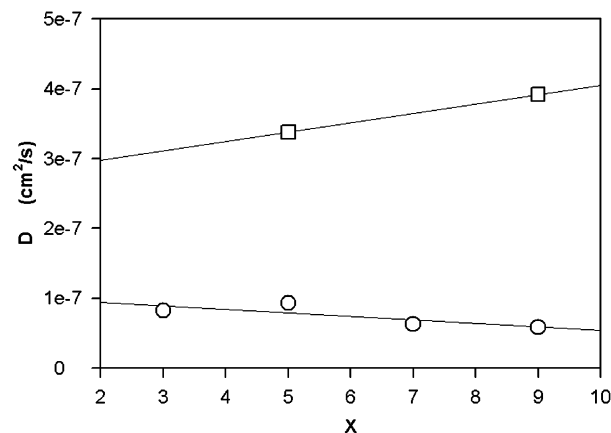


Figure 5. Transverse self-diffusion coefficient of Na^+ ions in sPI membrane measured by the radiotracer method versus the block size X for membrane with $\text{EW} = 792$ g/equiv (○) and membrane with $\text{EW} = 504$ g/equiv (□).

between D_{Tr} and the self-diffusion coefficient in dilute solution²⁸ are 0.03 ($\text{EW} = 504$ g/equiv) and 0.006 ($\text{EW} = 792$ g/equiv) for Na^+ ions ($D_0 = 1.30 \times 10^{-9}$ m²/s for Na^+), and they are 0.008 ($\text{EW} = 504$ g/equiv) and 0.001 ($\text{EW} = 792$ g/equiv) for $\text{N}(\text{CH}_3)_4^+$ ions ($D_0 = 1.18 \times 10^{-9}$ m²/s for $\text{N}(\text{CH}_3)_4^+$). The diffusion is greatly slowed in sPI membranes compared to unconfined solution. Several hypotheses can be put forward to explain this result: high tortuosity, very small size pores, strong interactions with the sulfonate group, presence of polymer chains in the hydrophilic pores, and others. A comparison with the widely studied Nafion membranes may give some answers. For the latter, the previous ratios were 0.15 for Na^+ and 0.015 for $\text{N}(\text{CH}_3)_4^+$ ions; this big difference had been assumed to be due to a steric aspect.²⁷ For sPI membranes, the ratio between D_{Tr} of Na^+ and D_{Tr} of $\text{N}(\text{CH}_3)_4^+$ is less important than that in Nafion membrane: it is equal to 4 ($\text{EW} = 504$ g/equiv) and to 6 ($\text{EW} = 792$ g/equiv), whereas it is equal to 10 for Nafion. This comparison suggests that the dimensions of the pore in sPI membranes is larger than that in Nafion membranes. The same conclusion was extracted from the small angle neutron and X-ray scattering (SANS and SAXS)²¹ studies, which suggests a typical size of scattering objects 5 times larger than that observed for Nafion. Another interesting point is that D_{Tr} and D_{Pr} values are small for both ions compared to other ionomer membranes.^{29,30} This phenomenon might then be ascribed to pathways filled with polymer chains that slow the transport of ions. This hypothesis is supported once again by SANS and SAXS experiments, which reveal a diffuse interface between hydrophilic and hydrophobic domains. Furthermore, electron spin resonance (ESR) studies³¹ reveal the whole water in sPI membrane is glassy. It is also supported by investigation on the degradation processes: for deteriorated membranes, the hydrophobic/hydrophilic domain interface becomes sharper and diffusion coefficient increases strongly. In addition, except for very large ammoniums ions, sPI membranes display a swelling dependency on the counterions²¹ much weaker than that with other ionomers. We have measured the amount of water in the membranes for both ions; it was approximately the same (see Table 2). Therefore, the swelling cannot be even partially responsible for the big difference between the D_{Tr} values measured for Na^+ ions and those measured for $\text{N}(\text{CH}_3)_4^+$ ions.

For all of the membranes studied here, a strong anisotropy of the transport properties (D_{Tr} , D_{Pr}) is observed. This anisotropy is more pronounced for the most weakly charged membranes: the ratio $D_{\text{Pr}}/D_{\text{Tr}}$ is about 10 for sPI of $\text{EW} = 792$ g/equiv, and

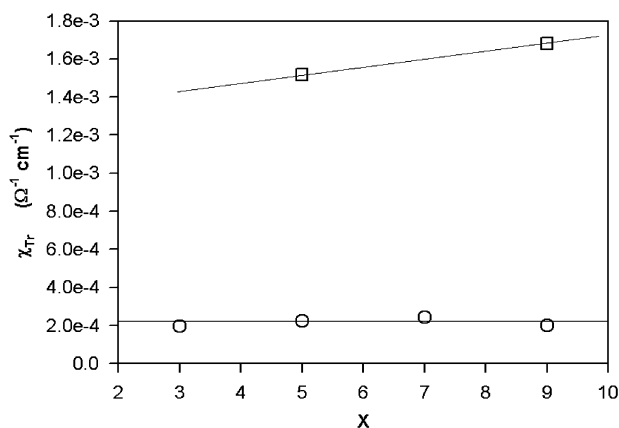


Figure 6. Transverse conductivity of $\text{N}(\text{CH}_3)_4^+$ ions in sPI membrane versus the block size X for membrane with EW = 792 g/equiv (○) and membrane with EW = 504 g/equiv (□).

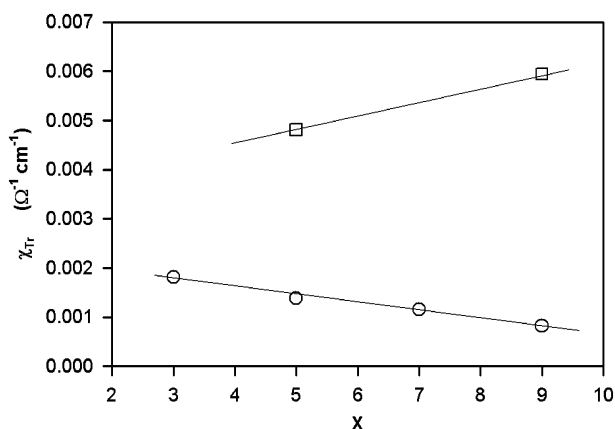


Figure 7. Transverse conductivity of Na^+ ions in sPI membrane versus the block size X for membrane with EW = 792 g/equiv (○) and membrane with EW = 504 g/equiv (□).

it is only about 3 for sPI of EW = 504 g/equiv. The influence of the ion content on the transport properties is only sensitive in the transverse direction suggesting continuous conductive pathways in the membrane parallel direction and an increase of the hydrophobic barrier in the transverse direction.

In the case of Na^+ ions, D_{Tr} seems to decrease versus X (see Figure 5), contrary to the case of $\text{N}(\text{CH}_3)_4^+$ ions where D_{Tr} seems constant versus the block size X . Depending on the counterions, we may or may not observe an influence of X on the transport.

3.3. Conductivity. Figures 6 and 7 represent the conductivity, χ_{Tr} , versus X for $\text{N}(\text{CH}_3)_4^+$ and Na^+ ions, respectively. The values χ_{Tr} exhibit a huge separation between the membranes of EW = 792 g/equiv and those of EW = 504 g/equiv; the ratio between these two sets of values is about 7 for $\text{N}(\text{CH}_3)_4^+$ ions and 4 for Na^+ ions. The influence of X is smaller than the one of EW. Upon increase of X , χ_{Tr} increases slightly for membrane of EW = 504 g/equiv with $\text{N}(\text{CH}_3)_4^+$ and Na^+ ions (Figures 6 and 7), remains constant for membrane of EW = 792 g/equiv with $\text{N}(\text{CH}_3)_4^+$ ions (Figure 6), and decreases for membrane of EW = 792 g/equiv with Na^+ ions (Figure 7).

The characteristic time scale of these conductivity experiments is about 10^{-5} s, whereas it is of tens of seconds for radiotracer experiments. The comparison of the results obtained by both latter techniques may give information on which scale the differentiation in the transverse transport properties occurs between the two membranes sets of different EW. As clearly seen in Figures 6 and 7, this difference occurs already at the

TABLE 2: Volume Fraction of Water, Φ_w , in sPI Ionomer Membranes for Na^+ and $\text{N}(\text{CH}_3)_4^+$ Ions^a

membrane	X	Φ_w (Na^+)	Φ_w ($\text{N}(\text{CH}_3)_4^+$)	Φ_w (H^+)
504	5	0.51	0.49	0.52
504	9	0.45	0.41	
792	3	0.42	0.40	0.39
792	5	0.43	0.42	0.40
792	7	0.47	0.42	
792	9	0.45	0.41	0.52

^a The values for H^+ are taken from the paper of Cornet et al.²¹

time scale of conductivity measurements, that is, at some 10^{-5} s. In other words, this means that the differentiation occurs at very local length, less than 100 nm ($L = (2Dt)^{1/2} = 1.4 \times 10^{-8}$ m with $D = 10^{-11}$ m²/s).

In the case of $\text{N}(\text{CH}_3)_4^+$ ions, no relevant variation of the conductivity χ_{Tr} versus X is noted as illustrated in Figure 6. However, in the case of Na^+ ions a decrease of χ_{Tr} versus X occurs (about 30%–40% rising from $X = 3$ to $X = 9$). The same behavior is noted in radiotracer and conductivity experiments. However, for Na^+ ions, there is a sharper decrease in χ_{Tr} in comparison to D_{Tr} . These results can be compared with those published by Cornet et al.^{21,32} on the same kind of sPI membrane neutralized by protons; they have observed an 80% decrease of χ_{Tr} . As it was suggested in the radiotracer results, the effect of X appears to be balanced by the counterion: the smaller the size, the stronger the effect of X . In addition, the variation of the water volume fraction Φ_w versus X (see Table 2) clearly indicates that this decrease of the transverse transport coefficients versus X is not due to the swelling properties of sPI membranes (for EW = 792 g/equiv sPI ionomer, Φ_w tends to increase with X). Although it is rather tricky to use the Nernst–Einstein relation ($D_i = \chi_i RT / (F^2 C_i)$) in an ion exchange membrane,³³ it has been shown in Nafion that the D_{Tr} deduced from this relation was equal to the D_{Tr} directly measured using a radiotracer technique.^{34,35} Therefore, it would be interesting to compare those two values; they are approximately equal in the case of sPI EW = 504 g/equiv, whereas they are separated by a factor of 2 in the case of sPI EW = 792 g/equiv, as it is reported in Table 1. This suggests that the polymer organization at local scale is rather different between the two ionic charge capacities. This point is supported by the particular dependence of the conductivity χ_{Tr} on EW: χ_{Tr} decreases when EW varies from 504 g/equiv to 613 g/equiv, then remains stationary until EW = 792 g/equiv, and then decreases again.²² For a sPI membrane that has an EW = 792 g/equiv, the local organization is probably stronger than the one of more highly charged membrane.

Another interesting comparison can be performed with the parallel self-diffusion coefficients (NMR): the self-diffusion coefficient in the transverse direction calculated from the Nernst–Einstein relation is smaller than the one in the parallel direction. This means that at the conductivity scale (around 10^{-8} m), an anisotropic structure slows the transport in the transverse direction. This anisotropic structure at the tens of nanometers scale deduced from the transport properties is in good agreement with the SAXS experiments that show anisotropic spectra.

Because of the decrease of the transverse transport coefficients versus X , it would then have been expected to have an increase of the parallel transport coefficient versus X . This behavior may be due to the foliated character of the sPI membrane structure.²² Indeed, a sponge-like three-dimensional structure (even anisotropic) leads to a three directional influence of the parameters and not bidirectional as observed for sPI membranes. If some

TABLE 3: Ratio of the Transport Coefficients (the Conductivity, χ_{Tr} , the Parallel Self-Diffusion Coefficient Measured by the PFGSE NMR Technique, D_{Pr} , and the Self-Diffusion Coefficient Measured by the Radiotracer Technique, D_{Tr}) for Membrane with EW = 504 g/equiv and with EW = 792 g/equiv for a Given X

X	$\chi_{Tr}(504)/\chi_{Tr}(792)$ Na ⁺	$\chi_{Tr}(504)/\chi_{Tr}(792)$ N(CH ₃) ₄ ⁺	$D_{Pr}(504)/D_{Pr}(792)$ N(CH ₃) ₄ ⁺	$D_{Tr}(504)/D_{Tr}(792)$ Na ⁺	$D_{Tr}(504)/D_{Tr}(792)$ N(CH ₃) ₄ ⁺
5	3.4	5.9		3.7	6.1
9	6.7	9.4	1.4	6.7	6

barrier induced a decrease of the transport in one direction, the probability to go in the two other directions would increase proportionally. At this point, it is difficult to reach a definite conclusion because of the weak variations observed with the N(CH₃)₄⁺ ions in both directions. It would be interesting to know whether the nondependence versus X observed in the parallel direction for N(CH₃)₄⁺ ions is true whatever the counterion is or whether it is a function of the counterion as we observed in the transverse direction. Unfortunately, because the relaxation times T_1 and T_2 of ²³Na are on the order of the milliseconds, it makes impossible the self-diffusion coefficient measurement by PFGSE NMR technique. The use of radiotracers is also impossible because the time needed for the experiment is too long (for a diffusion over 1 cm of membrane, it would last several months). A study with smaller ions would be more informative; Li⁺ ion appears to be a good candidate with respect to its size and NMR properties. The decrease of the transport versus X is more pronounced for χ_{Tr} than for D_{Tr} , that is, at local scale (100 nm, conductivity experiments) than at macroscopic scale (100 μ m, radiotracer experiments). One assumption that can be put forward to explain this difference is the following: The polymer arranged in folio packs²² is less organized between the packs. Indeed, in the conductivity measurements (i.e., nanometer scale), one follows the transport in the folios and in the region between the folios, but in radiotracer experiments one mainly follows the transport between the folio packs. The weaker influence of X at the micrometer scale seems to indicate that the passage from one pack to another is independent of X . Moreover, this effect is balanced by the nature of the counterion, particularly its size. They might explore different pathways according to their size: the smaller the ion, the more easily it can take narrow and more numerous pathways. This suggests a quite important polydispersity in the pore size. This phenomenon would also imply that the phase separation is not as sharp as that in perfluorinated ionomer membranes, like Nafion. As already mentioned in the radiotracer section, SANS, ESR, and degradation studies lead to the same conclusion. Besides, the transmission electron microscopy (TEM) experiments show that the electronic density variation is extremely low despite a well-defined foliated structure.²²

It is also interesting to look, for a given X , at the ratio of the transport coefficient when EW = 504 g/equiv over the one EW = 792 g/equiv (see Table 3). This ratio is the same for the conductivity and for the radiotracer measurements. This suggests that the charge concentration in the polymer chain influences the packing only at a local scale and not the foliated structure of micrometer characteristic size in terms of size, number, and arrangement.

4. Conclusion

Transport processes have been studied in sPI membrane in the direction parallel and transverse to the membrane surface using NMR PFGSE, radiotracer, and conductivity.

A strong anisotropy in the transport properties is observed. It is dependent on the equivalent weight of the membrane: the

more highly charged the membrane, the weaker the transport anisotropy. Depending on the counterion, the transverse transport slightly decreases as the length of the block X increases. At this point, the nature of this influence remains unclear.

The experimental results seem to indicate that the polymer is organized in a foliated structure with two characteristic scales: one about some tens of nanometers and one about the micrometer. Moreover, the polymer appears less organized between the folio packs. The representative volume of the structure has been estimated around 60–70 μ m³. The quantity of charges in the polymer chain clearly influences the structure: the more charged the membrane, the less strongly organized. The transport results confirm the presence of polymer chains in the hydrophilic pores, contrary to Nafion.

This copolymer appears to be an interesting material for studies on the relation between structure and transport properties although their preparation sensitivities make their study difficult. In particular, the distribution of charges, as well as the flexibility of the chain, can be controlled by changing the initial monomers.⁷ Indeed, the structural anisotropy is induced by the rigidity of sPI polymer chains.

Acknowledgment. We acknowledge the contribution of N. Prulière and J.-P. Simonin in the radiotracer experiments. We are deeply grateful to Armel Guillermo for his precious help on NMR experiments. The authors thank L. Rubatat for his help on conductivity measurements. We thank Ferdinand Volino and Patrice Porion in offering stimulating discussions. The authors are indebted to the Centre Grenoblois de Résonance Magnétique (CGRM) for providing the NMR facilities and the Laboratoire Liquide Ionique et Interfaces Chargées (LI2C) for providing the radiotracer facilities. The authors are indebted to the CNRS/LMOPS and Régis Mercier for polymer synthesis and to the CEA-Le Ripault, Philippe Capron, and Franck Jousse for the membrane preparation. This work has been supported by the French Ministry of Research and Technology through the PREDIT and “Réseau technologique PACo” programs. The authors are deeply indebted to Cathy Wague for her critical insight.

References and Notes

- (1) Schmeller, A.; Ritter, H.; Ledjeff, K.; Nolte, R.; Thorwirth, R. Eur. Patent EP 0574791 A2, 1993.
- (2) Kerres, J.; Cui, W.; Reichle, S. *J. Polym. Sci., Part A: Polym. Chem.* **1996**, *34*, 2421.
- (3) Genies, C.; Mercier, R.; Sillion, B.; Cornet, N.; Gebel, G.; Pineri, M. *Polymer* **2001**, *42*, 359–373.
- (4) Genies, C.; Mercier, R.; Sillion, B.; Petiaud, R.; Cornet, N.; Gebel, G.; Pineri, M. *Polymer* **2001**, *42*, 5097–5105.
- (5) Vallejo, E.; Pourcelly, G.; Gavach, C.; Mercier, R.; Pinéri, M. *J. Membr. Sci.* **1999**, *160*, 127–137.
- (6) Piroux, F.; Espuche, E.; Mercier, R.; Pinéri, M.; Gebel, G. *J. Membr. Sci.* **2002**, *209*, 241–253.
- (7) Fang, J.; Guo, X.; Harada, S.; Watari, T.; Tanaka, K.; Kita, H.; Okamoto, K. *Macromolecules* **2002**, *35*, 9022–9028.
- (8) Guo, X.; Fang, J.; Watari, T.; Tanaka, K.; Kita, H.; Okamoto, K. *Macromolecules* **2002**, *35*, 6707–6713.
- (9) Tanner, J. E.; Stejskal, E. O. *J. Chem. Phys.* **1968**, *4*, 1768–1777.
- (10) Wu, D.; Chen, A.; Johnson, C. S., Jr. *J. Magn. Reson. A* **1995**, *115*, 260–264.

- (11) Cotts, R. M.; Hoch, M. J. R.; Sun, T.; Markert, J. T. *J. Magn. Reson.* **1989**, *83*, 252–266.
- (12) Rollet, A.-L.; Simonin, J.-P.; Turq, P. *Phys. Chem. Chem. Phys.* **2000**, *2* (5), 1029.
- (13) Périé, M.; Périé, J. *Russ. J. Electrochem.* **1996**, *32* (2), 259–264.
- (14) N. Cornet, Ph.D. Thesis, Université J. Fourier, 1999.
- (15) Callaghan, P. T.; Coy, A.; Halpin, T. P. J.; MacGowan, D.; Packer, K. J.; Zelaya, F. O. *J. Chem. Phys.* **1992**, *97* (1), 651–662.
- (16) Callaghan, P. T.; Stepisnik, J. *Advances in magnetic and optical resonance*; Academic Press: 1996; Vol. 19, p 325.
- (17) Mitra, P. P.; Sen, P. N.; Schwartz, L. M.; Le Doussal, P. *Phys. Rev. Lett.* **1992**, *68* (24), 3555–3559.
- (18) Lteif, R.; Dammak, L.; Larchet, C.; Auclair, B. *Eur. Polym. J.* **1999**, *35*, 1187–1195.
- (19) Yeager, H. L.; Kipling, B. *J. Electrochem. Soc.* **1980**, *127* (2), 303–307.
- (20) Will, F. G. *J. Electrochem. Soc.* **1979**, *126* (1), 36–42.
- (21) Cornet, N.; Diat, O.; Gebel, G.; Jousse, F.; Marsacq, D.; Mercier, R.; Pineri, M. *J. New Mater. Electrochem. Syst.* **2000**, *3*, 33–42.
- (22) Blachot, J.-F.; Diat, O.; Putaux, J.-L.; Rollet, A.-L.; Rubatat, L.; Vallois, C.; Müller, M.; Gebel, G. *J. Membr. Sci.* **2003**, *214*, 31–42.
- (23) Latour, L. L.; Mitra, P. P.; Kleinberg, R. L.; Sotak, C. H. *J. Magn. Reson. A* **1993**, *101*, 342–346.
- (24) Seland, J. G.; Sorland, G. H.; Zick, K.; Hafskjold, B. *J. Magn. Reson.* **2000**, *146*, 14–19.
- (25) Duval, F. P.; Porion, P.; Faugère, A.-M.; Van Damme, H. *J. Colloid Interface Sci.* **2001**, *242*, 319–326.
- (26) Rollet, A.-L. Ph.D. Thesis, Université Pierre et Marie Curie, 1999.
- (27) Rollet, A.-L.; Simonin, J.-P.; Turq, P.; Gebel, G.; Kahn, R.; Noel, J.-P.; Vandais, A.; Malveau, C.; Canet, D. *J. Chem. Phys. B* **2001**, *105* (19), 4503–4509.
- (28) Mills R.; Lobo, V. M. M. *Self-diffusion in Electrolyte Solutions*; Physical Sciences Data 36, Elsevier: Amsterdam, 1989.
- (29) Mokrani, S.; Dammak, L.; Bulvestre, G.; Larchet, C.; Auclair, B. *J. Membr. Sci.* **2002**, *199*, 147–160.
- (30) Yeager, H. L.; Twardowski, Z.; Clarke, L. M. *J. Electrochem. Soc.* **1982**, *129* (2), 324–327.
- (31) Motyakin, M. V.; Cornet, N.; Gebel, G.; Schlick, S. *Bull. Pol. Acad. Sci., Chem.* **2000**, *48* (4), 273–292.
- (32) Cornet, N.; Beaudoin, G.; Gebel, G. *Sep. Purif. Technol.* **2001**, *22–23*, 681–687.
- (33) Poiteau, A. M.; Prigent, Y.; Chemla, M. *J. Chim. Phys.* **1975**, *72* (1), 57–65.
- (34) Pourcelly, G.; Sistat, P.; Chapotot, A.; Gavach, C.; Nikonenko, V. *J. Membr. Sci.* **1996**, *110*, 69–76.
- (35) Millet, P. *J. Membr. Sci.* **1990**, *50*, 325–328.